Thermodynamic pedodiversity patterns reveal higher-order soil organization in indigenous agroecosystems of the U.S. Southwest

Trevan Flynn[a,b*]

[a]Department of Agronomy, University of Fort Hare, Alice, 5700 South Africa

[b]Department of Research, add1Technologies, 11531 Slick Rock Dr., Richmond TX 77406 USA

Correspondence: t.flynn@add1technologies.com

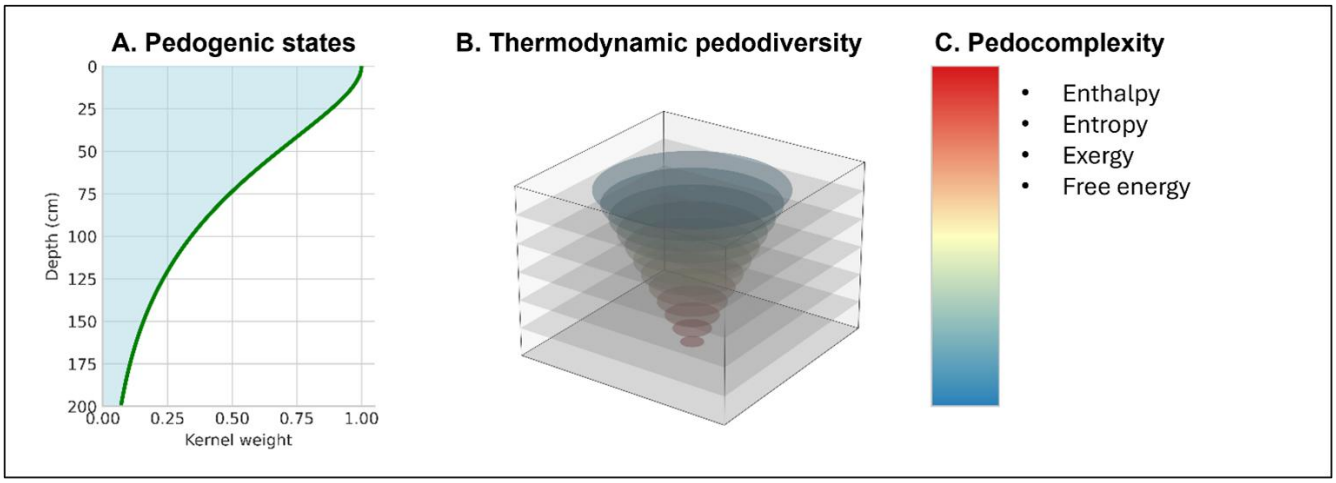

Abstract

Patterns of soil spatial heterogeneity and diversity support the stability and productivity of food systems, yet their multidimensional structure remains difficult to quantify at spatial scales relevant to agricultural resilience. A process-based framework grounded in fundamental physical principles is therefore needed to describe these spatial processes across landscapes. The aim of this study was to develop a mechanistic three-dimensional thermodynamic pedodiversity index constrained by physical continuity. The framework was applied to ancestral and contemporary indigenous agroecosystems of the U.S. Southwest. Eight gridded soil properties were transformed into thermodynamic exergy states using a three-dimensional biweight multi-pass convolutions applied across spatial directions, with the surface layer subject to atmospheric forcing. Local inverse Moran's I was then calculated to quantify the pedodiversity patterns. Linking thermodynamic principles to the landscape scale revealed that long-term crop production aligns with structured pedodiversity patterns rather than with pedodiversity magnitude alone. Persistent Hopi dryland agriculture corresponded with moderately to highly organized pedodiversity patterns, whereas more specialized Navajo pastoral systems occurred in landscapes characterized by lower pedodiversity organization. These results suggest that pedodiversity represents only one component of soil resilience and multifunctionality. Higher-order spatial processes, interpreted alongside indigenous ecological knowledge, are necessary to understand how soil supports sustained agroecosystems. Integrating process-based applied mathematics with Indigenous knowledge systems may therefore provide a pathway toward identifying higher-order functions such as pedocomplexity, capable of inferring soil resilience and multifunctionality.

Keywords: Exergy, Indigenous knowledge, Soil resilience, Soil multifunctionality, Quantitative pedology

1. Introduction

Soil is an inherently complex system shaped by the interaction of biological, chemical, physical (Jenny, 1941) and anthropogenic processes that operate across multiple spatial, depth and temporal scales simultaneously (Dearing et al., 2014). These processes generate a remarkable degree of variability both across the landscape and through the soil profile that are essential for ecosystem services such as water regulation, carbon storage and nutrient cycling (McBratney and Minasny, 2007). Understanding soil multifunctionality and resilience requires capturing the variability, a task that remains conceptually and methodologically challenging. The field of pedodiversity emerged to provide a quantitative framework for describing this heterogeneity and connecting it to ecological and pedogenic dynamics (Ibáñez et al., 1995).

Classically, pedodiversity has been quantified through the diversity of soil types (taxonomic), soil horizons (genetic) or soil productivity under different environmental changes (functionality)(Ibáñez and Bockheim, 2013). While valuable, these methods are constrained by their reliance on discrete taxonomic boundaries (Zhu, 1997) or rely on one purpose and thus fail to capture the continuous and multidimensional nature of soil variation, the interactions among soil attributes or rely on one attribute which does not reflect the true multifunctionality of soil (Toomanian and Esfandiarpoor, 2010). Accordingly, there is a need to calculate pedodiversity by recognizing that soil varies not only vertically with depth but also laterally across the landscape, and that processes occurring

within one profile can influence the functionality of neighbouring soil and horizons (Matheron, 1963).

In the U.S. Southwest, soil preserves a long record of interactions between people, agriculture and climate. The Ancestral Pueblo, Navajo and Hopi (among many others) agricultural systems developed under extreme climatic constraints, relying on detailed ecological knowledge and a profound understanding of soil heterogeneity to sustain crop production over centuries during extreme climatic events. For instance, the cultural and trading center of Chaco Canyon likely imported food from the Chuska Mountains to the west, where maize, beans and squash could be cultivated (Benson et al., 2003). In Mesa Verde, agriculture was primarily conducted on the mesa tops and extended northward into the Great Sage Plains, which were extensively cultivated by the late era of the Ancestral Pueblo (Benson, 2011). Yet, it remains unclear whether these lands were chosen for their extensive homogeneous, high-quality soil or for their spatially heterogeneous variation, which may have offered greater adaptive opportunities under varying climatic conditions.

The Hopi, considered possible cultural descendants of the Ancestral Pueblo have practiced dryland farming for at least nine centuries, since around 1,100 A.D. (Bocinsky and Varien, 2017), possibly following the decline of Chaco Canyon. Their agricultural system exemplifies an enduring strategy that capitalizes on pedodiversity, intentionally seeking sites that differ from the surrounding landscape to maximize functional diversity and resilience. The Hopi territory represents one of North America's longest-inhabited agricultural landscapes (Johnson, 2023) and a recognized biodiversity hotspot (Nankar and Pratt, 2021), shaped by cultural practices that exploit soil variability, crop diversity through selective breeding and has lasted through extreme drought. For example, the Hopi cultivate 17 distinct drought-resistant nutrient dense maize

varieties, an exceptional adaptation given maize's typical dependence on abundant water (Soleri and Cleveland, 1993).

By continuously quantifying pedodiversity, we can reveal how this intrinsic, multidimensional soil complexity supports the persistence of traditional dryland farming systems (Mikhailova et al., 2021). High vertical pedodiversity reflects the development of layered soil profiles or profiles with discrete boundaries, whereas spatial pedodiversity represented the by spatial heterogeneity (i.e., squared differences) of niches historically exploited for distinct crops, breeding and management strategies. Mapping these interconnected domains simultaneously shows landscapes where agricultural traditions have upheld ecological balance and soil functionality across generations (Costantini and L'Abate, 2016). Conversely, such analyses may also reveal agricultural strategies that favored lower pedodiversity and greater soil homogeneity in areas possessing inherently favorable soil and moisture regimes.

The aim of this study was to quantify a process-based, numerical second-order voxel index to characterize the pedodiversity of soil thermodynamic states, providing insight into community-level soil behavior. Applied across Ancestral Pueblo agricultural landscapes and multigenerational dryland farming regions of the U.S. Southwest, we show that thermodynamic pedodiversity or soil system organization, forms part of a framework for assessing soil resilience and societal adaptation to environmental stress. By capturing physical properties, spatial structure and depth organization, this approach offers a rigorous measure of soil arrangements and an ecological–cultural perspective for understanding how human management practices have persisted, adapted and transformed under variable environmental conditions.

2. Methods and materials

2.1 Sites

The Four Corners region of the U.S. southwest and the three sites chosen were selected because they represent the agricultural and cultural legacies of the Ancestral Pueblo, Navajo and Hopi peoples (Brooks, 2020) whose histories are interrelated through geography yet are culturally distinct (Figure 1). Although the Navajo and Hopi occupy regions that overlap with former Ancestral Pueblo territories and each other, their languages, cultural practices and agricultural systems differ significantly (Dongoske et al., 1997; Kahn-John (Diné) and Koithan, 2015). For this reason, and in recognition of their unique cultural identities and histories, the Navajo and Hopi are distinct from the Ancestral Pueblo. The cultural history of the region is further complicated by overlapping territorial boundaries; for example, Hope Land lies within the Navajo Nation, yet the two peoples maintain separate cultural traditions. Additionally, the term “Anasazi”, historically used in archaeological literature to refer to the Ancestral Pueblo is now avoided due to its derogatory meaning, “ancient enemy,” (McBrinn and Cordell, 2016) in Diné Bizaad (the Navajo language). Whether this term originated as a Western construct or was relayed to archaeologist Richard Wetherill, who popularized it, remains uncertain, but its use highlights the importance of cultural sensitivity and self-identification in interpreting the human history of the U.S. Southwest.

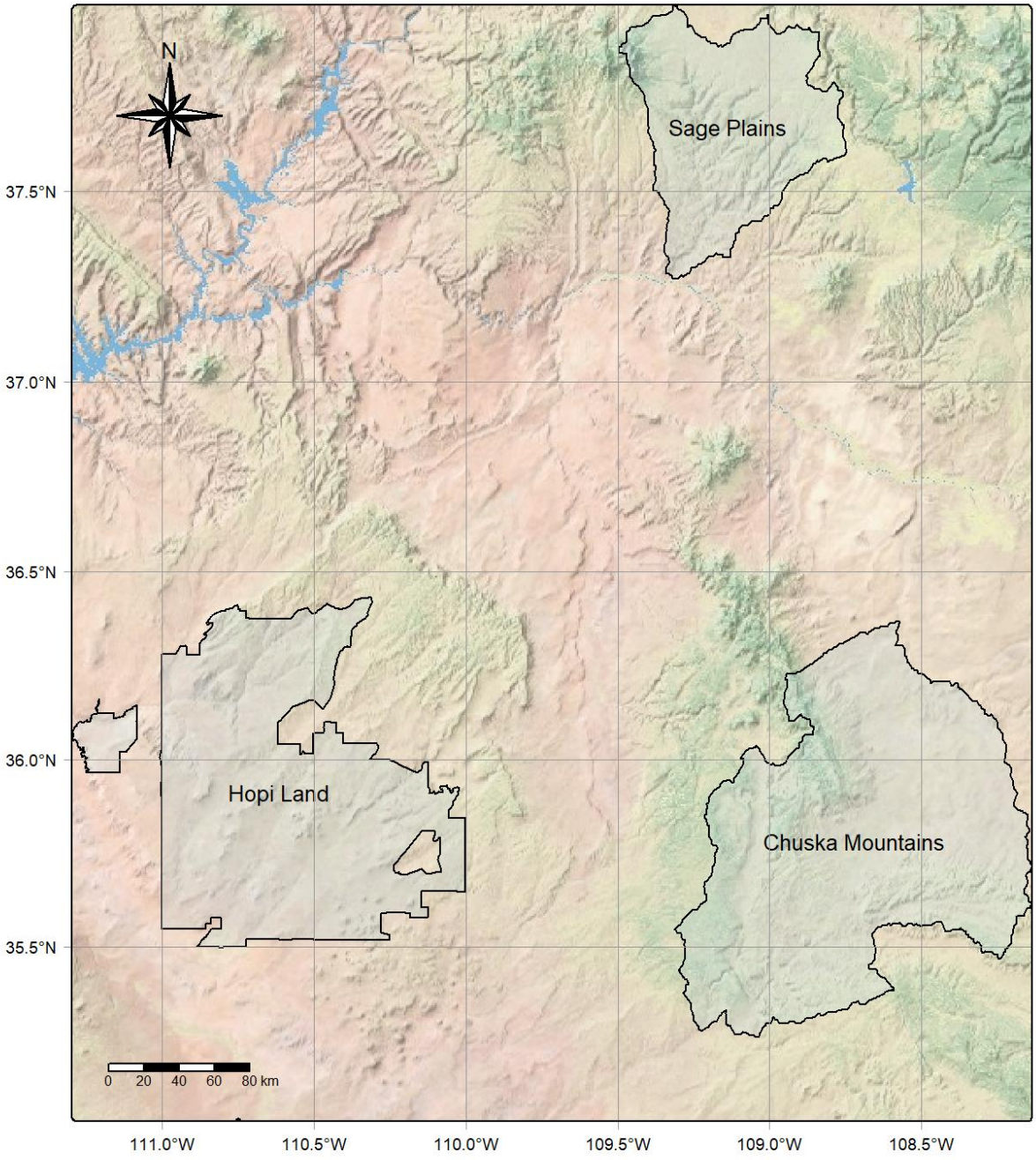

115

116 *Figure 1: known indigenous lands selected based on borders or basins due to water resources, which likely determined their*
117 *agriculture practices.*

118 Except for Hopi Land, the sites were delineated primarily from hydrological basins identified

119 through a digital elevation model (DEM), crossing state boundaries (Colorado, Utah, Arizona and

120 New Mexico). This geomorphic criterion was chosen because, although some ancestral cultures

constructed irrigation networks, all ultimately relied on dryland agriculture (Bellorado and Anderson, 2013). Basins or catchments, concentrate runoff and moisture and thus represent the most probable zones of Ancestral Pueblo cultivation. Site selection also considered the spatial distribution of early and late Ancestral Pueblo agricultural landscapes and their overlap with the territories of contemporary Indigenous peoples. While this spatial correspondence is inherently interpretive, it reflects well-established archaeological and ethnogeographic evidence that the Ancestral Pueblo peoples inhabited and farmed across the Four Corners region of the U.S. Southwest.

2.1.1 Chuska Mountains

The southern Chuska Mountains, southern basin and its piedmonts, straddling the Arizona–New Mexico border, form a volcanic highland rising above the surrounding Colorado Plateau. The range is composed primarily of Oligocene basaltic and andesitic flows (Appledorn and Wright, 1957), interbedded with volcaniclastic sandstones and Chuska Sandstone, underlain by older Mesozoic sedimentary formations such as the Navajo and Wingate Sandstones. Elevation ranges from approximately 1,800 to 2,900 m, with the southern basin averaging 2,053 m (Blagbrough, 1967). Vegetation transitions sharply from montane forests of ponderosa pine, spruce and fir at higher elevations to pinyon–juniper woodland and semi-arid grassland across the lower slopes and basins (Harris et al., 1960). The climate spans alpine to desert conditions, characterized by cool, snowy winters and warm, dry summers, with precipitation varying from >500 mm yr^{-1} on the crest to <250 mm yr^{-1} in the southern lowlands (Blagbrough, 1967). Culturally, this region was a critical resource and agricultural hinterland for Chaco Canyon (~900 AD), supplying timber and agricultural products to the Ancestral Pueblo (Wills et al., 2014). The same landscapes are

traditional herding and grazing grounds of the Navajo Nation, whose pastoral systems continue to shape soil use and vegetation patterns (Wallace et al., 2021).

2.1.2 Great Sage Plain

The Great Sage Plains lies north of Mesa Verde and west of the Dolores River in southwestern Colorado and southeastern Utah, forming part of the northern San Juan Basin margin. The landscape consists primarily of Cretaceous Mancos Shale overlain by Quaternary loess, alluvium and colluvial deposits, with minor outcrops of the Dakota Sandstone and Mesa Verde Group along drainage margins (Reheis et al., 2018). The average elevation is 2,050 m, with a gently undulating topography that contrasts sharply with the dissected mesas to the south (Dove et al., 2006). Soil is predominantly fine-textured loams and clay loams, developed on shale and loess parent materials that provide high moisture retention but limited infiltration (Fadem and Diederichs, 2020). The regional climate is semi-arid continental, with cold winters, warm summers and mean annual precipitation of 300–400 mm, much of it derived from winter snowmelt. Vegetation is dominated by sagebrush steppe, greasewood and semi-arid grassland, interspersed with dryland agricultural fields (Wagner and Scipal, 2000). Archaeologically, this area marks the northern agricultural frontier of the Ancestral Pueblo world, cultivated most intensively between 1000 and 1280 A.D., (Allison, 2010).

2.1.3 Hopi Land

The Hopi Mesas occupy a prominent series of east–west–oriented uplands in northeastern Arizona, rising above the northern edge of the Little Colorado River Basin. The landscape is underlain by Jurassic and Triassic sandstones, principally the Entrada, Wingate and Navajo Sandstones interbedded with minor siltstone and shale that create subtle contrasts in soil texture

and water-holding capacity (O'Sullivan, 2003). Elevation ranges from approximately 1,700 to 1,900 m, and the region's arid to semi-arid climate is characterized by mean annual precipitation of 200–300 mm, concentrated during the summer monsoon, with mean annual temperatures of 10–13 °C (Hopi Department of Natural Resources, 2021). Vegetation is mostly pinyon–juniper woodland, sagebrush and mixed grassland, with riparian shrubs in ephemeral washes. The region forms one of North America's oldest continuously farmed landscapes, where the Hopi people have practiced dryland agriculture for over nine centuries. Their fields, often situated on mesa slopes and valley bottoms, support a remarkable diversity of drought-tolerant maize, beans, squash, melons and medicinal plants (Johnson et al., 2021; Wall and Masayesva, 2004).

2.2 Soil data

Soil property data was obtained from the POLARIS (Probabilistic Remapping of SSURGO) dataset (Chaney et al., 2016). and the USDA-NCSS soil survey data (SSURGO back-filled with STATSGO where SSURGO is not available) database (Walkinshaw, 2020), both providing harmonized, gridded soil property estimates across the conterminous United States. POLARIS was used to represent the physical soil matrix, while USDA-NCSS soil survey supplied soil color data critical for redox-morphological interpretation (Kim et al., 2025). All soil properties were obtained within the Google Earth Engine (GEE; Gorelick et al., 2017) to streamline the modelling process.

The POLARIS dataset provides probabilistic predictions of major soil attributes at a 30 m spatial resolution (Chaney et al., 2016). Seven properties were extracted for this study: bulk density (g cm^{-3}), sand (% w/w), silt (% w/w), clay (% w/w), saturated hydraulic conductivity (K_{sat}; $\log_{10}$(cm hr^{-1})), soil organic matter ($\log_{10}$(% w/w)) and pH. Each property was available at the six standard GlobalSoilMap (Arrouays et al., 2014) depth intervals: 0–5, 5–15, 15–30, 30–60, 60–100 and 100–

200 cm. All soil properties were retained in their transformed state; for example, K_{sat} and soil organic matter were kept in their $\log_{10}$-transformed form, as their distributions are typically right-skewed and approximate normal after transformation (Shapiro et al., 1968; Webster and Oliver, 2007). This approach also preserves the proportional relationships among properties, which is preferable for kernel-based weighting and correlation analysis (McBratney et al., 1992).

Soil color acts as a morphological proxy for oxidation–reduction and drainage conditions, it was included as an eighth property to enhance the interpretability of the pedodiversity index. Munsell soil color data were resampled to 30 m spatial resolution using a nearest-neighbor approach to preserve the native fine-scale texture of the dataset. Depth intervals were retained in their original form, as the 3-dimensional kernel weights were designed to account for cross-layer influence of soil color at 10, 25, 75, and 125 cm.

2.3 Thermodynamic pedodiversity

2.3.1 Pedocomplexity theory

Thermodynamic pedodiversity is a key element of pedocomplexity, a framework that integrates soil thermodynamic states, continuous diversity, total potential energy and practical tools (e.g., decision-support) to evaluate soil resilience and multifunctionality. It emphasizes that pedodiversity alone cannot serve as a proxy for soil functionality, and that soil multifunctionality is instead governed by pedocomplexity. Pedocomplexity is a function describing the thermodynamic steady-state of soil, from which, using a multidisciplinary approach, soil resilience and multifunctionality can be inferred. Pedocomplexity is comprised of four components (Table 1).

Table 1: The components, steady state term and physical meaning of pedocomplexity.

Component	Steady state	Physical meaning
Latent energy	Enthalpy (ΔH)	The total stored energy in the system (useable + unusable).
Pedogenic states	Exergy (Ψ)	The magnitude of internal energy available for work (usable energy in the soil).
Pedogenic exchange	Entropy (σ)	The coupling or interaction energy dissipated to maintain gradients between pedogenic states.
Pedocomplexity	Organization of exergy (O)	A function of H, Ψ and σ describing the thermodynamical organization of the soil system

When defined for the whole system pedogenic states can be described as magnitude or intensity and pedogenic exchange can be shown as a thermodynamic pedodiversity index. The framework recognizes that soil always exists in a multidimensional physical and feature state. However, the term "pedogenic" is emphasized as a descriptor of process-based functions culminating in pedocomplexity, calculated as:

$$O(s) = \int f\colon \mathbb{C}(\Delta H, \Psi, \sigma)_{x,y,z,t}\, dV,$$

Or if the data is sparse, non-continuous or simply not enough data:

$$O(s) = \int f(\Delta H, \Psi, \sigma)_{x,y,z}\, dV$$

Where latent energy corresponds to enthalpy ΔH, representing total stored energy. This can be seen as uncertainty because a part of it is not exergy or useable for work. Pedogenic states are equivalent to exergy Ψ, capturing the usable internal energy available for work. Pedogenic exchange acts like entropy σ, representing the interaction energy dissipated to maintain spatial gradients between states. Finally, pedocomplexity (O) is a function of ΔH, Ψ and σ, describing the

overall thermodynamic structure of the soil system organization. In other words, the causality of storage, transformation and release of soil constituents.

Since exergy states assume a reference state, here it corresponds to a zero gradient representing no soil or the end of soil formation as the limits of a soil's life span. Consequently, a zero gradient is assumed to indicate zero functionality and no resilience to change, and the behavior determines which functions are expressed. Additionally, it implies boundary conditions at the surface of the soil column. Although this implicitly indicates linearity in time and ΔH, the model is not linear in these controls.

The σ function is fundamental for calculating pedocomplexity as defined here and the least understood. Pedogenic states and pedodiversity represent two distinct and often conflicting objective functions. While Ψ represents magnitude or a convergence process (e.g., the sum of exergy across dimensions), σ represents dissipation of energy, which is a divergent process (e.g., the covariance of exergy across dimensions). Although treating the problem as a voxel increases the degrees of freedom relative to unknown parameters, the conflicting objective functions exert a stronger influence and numerical stability drops significantly.

Perhaps most importantly, these conflicting loss functions can create visualizations that appear unrealistic despite mathematical stability, resulting in an effective function that is difficult to interpret and limiting its accessibility. A concept highly emphasized in the framework is keeping everything interpretable and easy to visualise. Consequently, we also want to create an index for σ and thus, thermodynamic pedodiversity, which is σ scaled [0,1] or the process from [0,1]. Although they are equivalent, it is important when mapping large regions depending on software or environment used. Therefore, to solve $O(s)$, σ must be an energy-minimizing function that

increases (not decreases) across dimensions yet defines the spread and never falls below zero, much like the spatial lag of variance, not covariance.

2.3.2 Profile to landscape scale

A mechanistic, multi-dimensional pedodiversity index was developed to represent the energy transfer dynamics that regulate soil state dissipation energy. The index integrated eight gridded soil properties across depth layers (image bands) using 3-dimensional biweight convolutions constrained by physical continuity. This expresses pedodiversity as a coupled spatial–vertical phenomenon, where spatial patterns of heterogeneity emerges from lateral and depth-dependent interactions among soil properties (Ibáñez and Bockheim, 2013). Although not a direct measure of soil functions, the index captures the organization and connectivity of exergy that is the foundation to soil multifunctionality (Bünemann et al., 2018; Vogel et al., 2018). The process is straightforward and can be represented schematically in linear form (Figure 2).

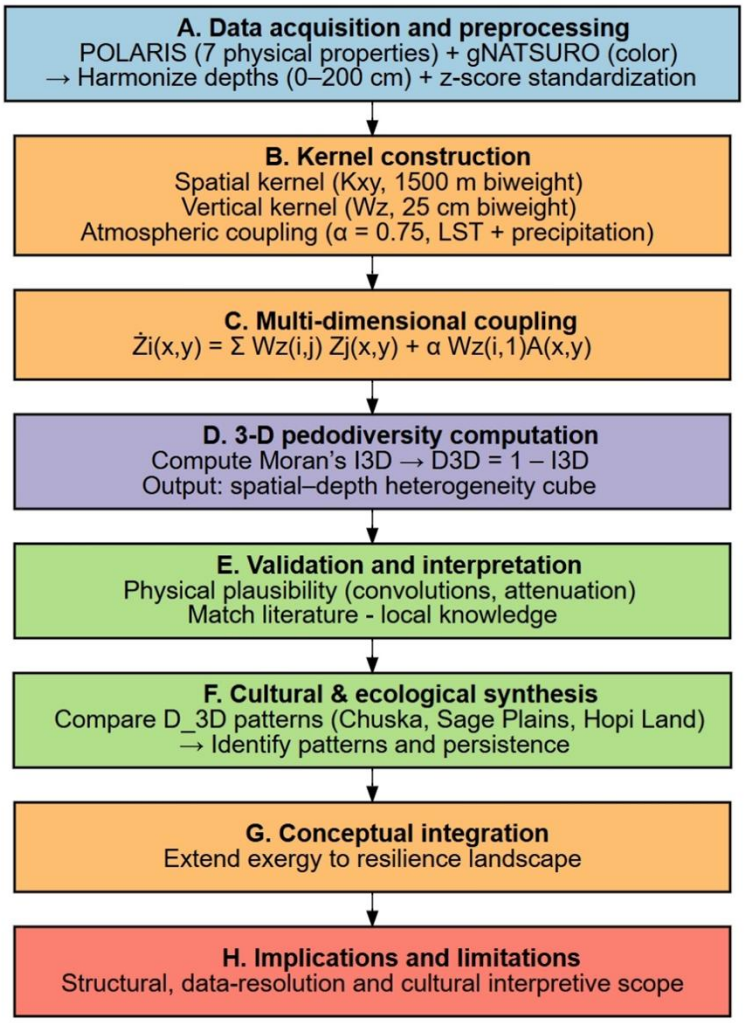

Figure 2: flowchat of the incorporation of the thermodynamic pedodiversity into the larger synthesis of agroecosystem resilience.

The complete pedodiversity computation, local mean and covariance calculations and normalization of the three-dimensional Moran's I (Moran, 1950) was implemented entirely in the GEE Python API. This approach ensured computational scalability across all properties and depths, allowing the calculation of the pedodiversity directly from a spatially harmonized soil property cube (Figure 3). This represents a new methodological application of GEE, as it is rarely used for depth-dynamic or three-dimensional subsurface analyses, extending its capacity beyond traditional two-dimensional surface modeling.

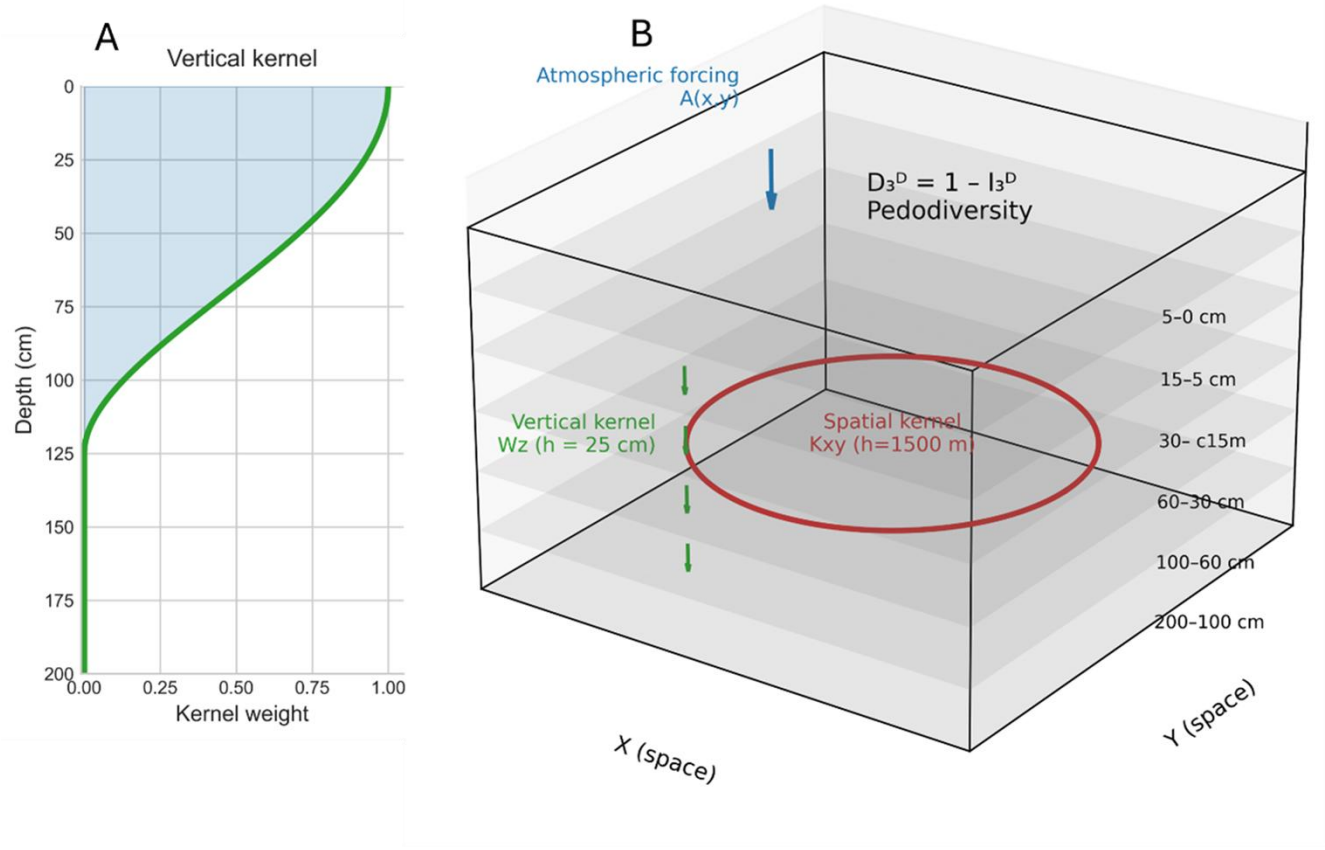

Figure 3: (A) Vertical curve generated from the biweights, illustrating depth-dependent coupling within the soil profile. (B) Spatial–vertical soil cube with atmospheric forcing $A(x, y)$. Together these components generate multidimensional coupling curves at each pixel, from which the pedodiversity index $D_{3D} = 1 - I_{3D}$ is calculated through the inverse of the three-dimensional Moran's I.

2.3.3 Three-dimensional convolutions

Although the thermodynamic pedodiversity index was implemented as an integrated framework, the spatial and vertical convolutions were computed independently and then merged into one. This separation provided diagnostic insight into the relative weighting along each dimension, allowing the model to be fine-tuned toward physical realism and to extract validation information. The vertical component operates over millimeter- to centimeter-scales, whereas the spatial component extends over meter- to kilometer-scale gradients. The local horizontal and vertical interactions between pixels were modeled using a biweight convolution function defined as:

$$K_{xyz}(\mathrm{d}) = \begin{cases} [1-(d/h)^2]^2 & d > h \\ 0, & d < h \end{cases}$$

where d is the Euclidean distance in the vertical domain (K_z) and the spatial domain (K_{xy}), while h is the bandwidth determining the maximum range of interaction. Both domains were subsequently normalized so that their integrated weights summed to one. This gives an almost symmetrical convolution, except where atmospheric forcing modified the weighting at the soil surface. The weights were combined through matrix algebra when implementing the algorithm. The biweighting was used because it provides a smooth, finite-support weighting function that emphasizes local interactions (Beaton and Tukey, 1974; Hengl et al., 2004), while preventing long-distance artifacts (Press, 2007).

2.3.4 Atmospheric boundary

Many soil depth functions have considered how to handle boundary conditions of the profile. While an exact analytical spline will solve this boundary problem, additional functions can be used if atmospheric forcing is applied, soil profile exergy never becomes zero gradient and may have implications for things like numerical classification pedocomplexity.

Since the topsoil forms the physical boundary of many atmospheric–pedologic interactions (e.g., infiltration, evaporation and heat exchange), an atmospheric forcing term $A(x, y)$ was introduced as a boundary condition:

$$\tilde{Z}_i(x, y) = \sum_{j=1}^{n} W_z(i, j) Z_j(x, y) + \alpha\, W_z(i, 1) A(x, y)$$

where $Z_j = X_j - \bar{X}$ represents deviations of soil property X_j from its mean, α is the coupling coefficient controlling the magnitude of atmospheric influence and $W_z(i,1)$ diffusion through the surface to lower depths. This formulation is like the Robin boundary condition (Gustafson and Abe, 1998), which combines flux and state terms to represent the exchange of energy or mass across boundaries. Here, it allows surface energy and moisture fluxes to be transported, stored and transformed through the soil profile, linking atmospheric variability directly to sub-surface processes.

2.3.5 Objective function

The objective function used in this study equates to the inverse 3-dimensional Moran's I. Which is the process that scales to [0,1] and can be used as an index and the pedogenic exchange loss function in pedocomplexity. However, it needs to be accumulating at each pixel and energy minimizing. Additionally, the function must calculate the patterns of spatial heterogeneity where it essentially collapses back into an energy form. This effectively makes it consistent in the framework, the spatial lag of variance represents pedodiversity and increases computation as the function simplifies.

For the objective function, we need the interaction energy density where local interactions accumulate:

$$E = \frac{1}{V}\sum_{i,j} J_{ij} s_i s_j$$

Where s is the variable state, J_{ij} is the coupling strength between the two states normalized by the volume. When defining the local Moran's I for the 3-dimensional convolution (I_3) and reframing it for energy dissipation, we get thr equation:

$$\sigma(x,y) = 1 - (I_3) \; = 1 - \frac{\sum_{i=1}^{n} \tilde{Z}_i(x,y)\, \tilde{Z}_{i,local}(x,y)}{n \cdot Var(X)(x,y)}$$

Here, $\tilde{Z}_{i,\text{local}}$ represents the horizontal mean of the standardized property, $\tilde{Z}_i$ using the spatial weights and $Var(X)$ denotes the local variance computed across depths (n) within the vertical weights.

Related to the interaction energy density, the $\tilde{Z}_{i,local}$ interacting state, the $\tilde{Z}_i$ the state variable and normalized by $n \cdot Var(X)$. As we are calculating the from the data over the dimensions, summation calculates the strength of coupling. Most importantly, it collapses back to a Dirichlet energy when summed across space.

$$\mathrm{E} \; = \int |\nabla Z|^2 dx$$

Thus, fitting the requirements for the thermodynamic pedodiversity objective function within the broader context of pedocomplexity.

The pedocomplexity objective function would ideally be linear solvable. However, the inverse Moran's I equation is deterministic and computationally efficient. Therefore, it could be used as an interpretable index and used in a more complex function to solve pedocomplexity, thus lowering the computational cost for large areas. This makes it ideal for both an index and for later computation as it solves the process and is visually interpretable without manipulation.

2.3.6 Implementation

The framework was implemented in GEE to ensure computational scalability across large spatial extents. The pedodiversity index was computed using a soil property image cube harmonized to six standard depths. The soil properties were all converted to global z-scores per depth, where the

mean equals 0 and standard deviation equals 1. Global z-scores were used to ensure each property contributes equally, scale invariant and to ensure physical meaning.

The horizontal domain had a maximum range of $h_m = 1{,}500$ m with a radius of 7 pixels and a spatial scale of 30 m, representing lateral field–to–field influence distances. The vertical domain used $h_z = 25$ cm as the effective correlation length between soil horizons, consistent with observed horizon thicknesses and infiltration depths. Atmospheric coupling ($\alpha = 0.75$) was applied only to the surface horizon to simulate boundary energy fluxes driven by surface temperature or precipitation and releasing exergy. Land surface temperature was obtained from cloud-masked Landsat 8 and 9 (USGS, 2021) imagery using the median composite for 2024, while precipitation data were obtained from NASA's Global Precipitation Measurement (GPM) mission, specifically the Integrated Multi-satellite Retrievals for GPM (IMERG) product (Huffman et al., 2023), by summing the total precipitation for the year 2024.

2.4 Validation and evaluation

Both quantitative and qualitative analyses were conducted on the multi-dimensional pedodiversity index. Quantitatively, we evaluated how the vertical, spatial and atmospheric coupling components behaved in physically plausible ways and how much of the observed variation was explained by intrinsic soil properties. Qualitatively, we examined whether the patterns identified by the index aligned with documented traditional practices, drawing on local dryland farming literature, anthropological studies and Indigenous ecological knowledge of the region. Integrating these perspectives was essential to interpret the pedodiversity patterns within their cultural and environmental context and without such knowledge, our understanding of the

358 past and present soil conditions remains incomplete, and our ability to adapt to future climate
359 change is fundamentally limited (Whyte, 2013).

360 3 Results and discussion

361 We developed a thermodynamic pedodiversity index that integrates eight soil properties along with
362 their depth continuity through a 3-dimensional convolution to quantify soil state pedodiversity
363 across multiple scales. This approach treats pedodiversity as an energy-density distribution,
364 capturing how exergy gradients are arranged and dispersed throughout physical space. By moving
365 beyond layer-based or taxonomic frameworks, this multidimensional method provides a
366 mechanistic representation of soil structure, offering a foundational perspective on soil systems
367 and the management decisions shaping diverse agroecosystems in the U.S. Southwest.

368 3.1 Vertical and spatial structure

369 The convolutions revealed a strongly stratified pattern of soil energy exchange. The upper 5–30 cm
370 formed the dominant zone of vertical coupling (Table 2), acting as an interface where atmospheric
371 interactions, anthropotropic activity, organic matter inputs and bioturbation generate high spatial
372 heterogeneity. Below ~60 cm, the strongly decoupled state reflects a shift toward a
373 thermodynamic and structural steady state, where minimal energy exchange preserves inherited
374 contrasts in texture and compaction, and biological contributions to surface-driven ecosystem
375 functions are greatly reduced (Wang, 2010). These deeper layers exert long-term influence on
376 rooting depth and drought buffering but play a smaller role in short-term cultivation dynamics.

377 *Table 2: Vertical weight bisquared matrix from purely soil properties*

	0-5 cm	5-15 cm	15-30 cm	30-60 cm	60-100 cm	100-200 cm

0-5 cm	0.511	0.423	0.066	0	0	0
5-15 cm	0.436	0.418	0.235	0	0	0
15-30 cm	0.075	0.325	0.579	0.021	0	0
30-60 cm	0	0	0.035	0.965	0	0
60-100 cm	0	0	0	0	1	0
100-200 cm	0	0	0	0	0	1

When atmospheric forcing was incorporated through land-surface temperature and precipitation coupling at the surface boundary, the convolution emphasized the 5–15 cm horizon as the primary energy mediator rather than the boundary 0-5 cm layer (Table 3). This suggests that the topsoil acts as a rapid transient layer, whereas the subsurface horizon functions as the primary buffer, storing and redistributing moisture and heat with delayed release acting as a stabilizing feature in drought-prone agricultural systems. Nevertheless, the 0–5 cm layer can shift to a primary energy-input zone for water and nutrients during germination, illustrating how soil multifunctionality emerges dynamically in response to plant establishment in dryland systems.

Table 3: The combined vertical weights incorporating influences from the atmosphere and the soil.

	0-5 cm	5-15 cm	15-30 cm	30-60 cm	60-100 cm	100-200 cm
0-5 cm	0.239	0.658	0.103	0	0	0
5-15 cm	0.137	0.552	0.311	0	0	0
15-30 cm	0.024	0.344	0.611	0.022	0	0
30-60 cm	0	0	0.035	0.965	0	0
60-100 cm	0	0	0	0	1.000	0
100-200 cm	0	0	0	0	0	1.000

Spatial convolution patterns further reinforced this structure (Figure 4): high surface connectivity, peak process diversity at intermediate depths and reduction toward deeper horizons. Functionally, this identifies the zone of maximum agricultural responsiveness, the horizons most critical for crop establishment, root exploration and moisture capture in arid environments. It should be noted that

the convolution weights represent the relative intensity of vertical and lateral energy exchange; however, a single convolution configuration was applied uniformly across all sites.

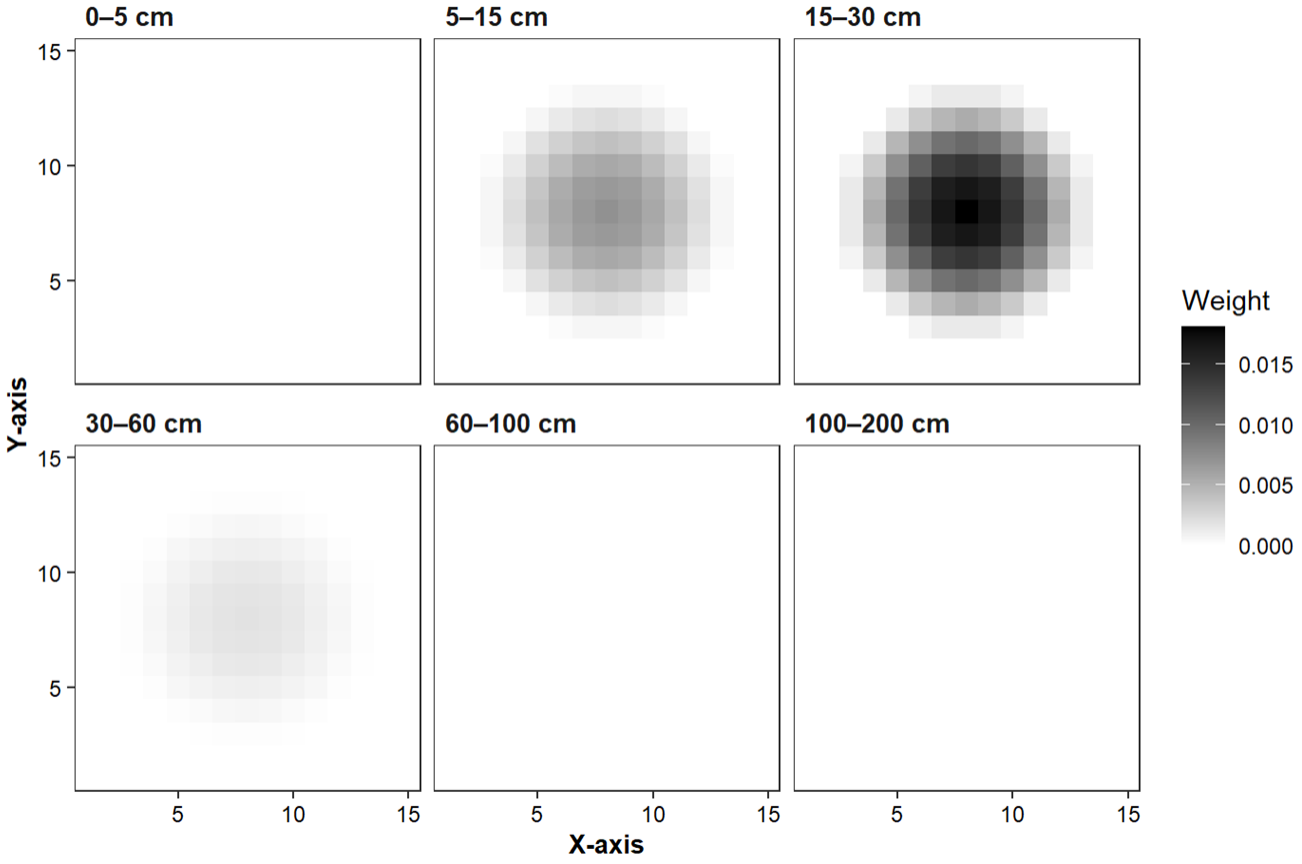

Figure 4: spatial and vertical interactions, note that there is a kernel applied through all depths, and this shows where the energy appears to be interacting.

The observed differences among depth layers arise from the soil property distributions themselves rather than from learned or adaptive convolution weights as used in deep learning or neural network architectures. In this framework, the convolution acts as a physics-informed coupler, not a data-trained filter, allowing soil heterogeneity relevant to exergy potential to emerge directly from the underlying soil matrix. Figure 4 illustrates the base convolution form and how its interactions reveal shifts in soil characteristics to soil processes across the landscape.

3.2 Spatial interpretation

The pedodiversity index align closely with areas historically associated with Ancestral Pueblo agriculture and long-term resilient farming traditions, reinforcing the connection between soil heterogeneity and adaptive land management (Pawluk, 1995). However, when interpreting a second-order voxel diversity index, it is important to recognize that higher values represent greater diversity in soil exergy states and composition, not necessarily more favorable conditions for a specific function or crop. In this context, pedodiversity reflects the potential for resilient outcomes rather than a direct measure of fertility or productivity (Handayani and Prawito, 2010). In other words, it represents the variety of choices present at a given location.

3.2.1 Chuska Mountains

The southern Chuska Mountains, the southern basin and its piedmont (Figure 5) span lands long inhabited by the Navajo peoples, where the soil and landforms have shaped, and been shaped by, diverse land use traditions (Pawluk, 1995). Along the northeastern slopes and piedmonts, soil of high pedodiversity (>0.50) developed where volcanic and sandstone parent materials merge through colluvial–alluvial processes across steep topographic gradients (Reneau et al., 1996; Seager et al., 1987). This heterogeneity, combined with contrasting moisture and temperature regimes, created many ecological niches from the timbered ridges to the cultivated footslopes once supporting maize, bean and squash gardens connected to the Chaco Canyon network (Doolittle, 2000; Vivian and Hilpert, 2012). At higher elevations, timber resources rather than

agriculture dominated, with the diversity of soil reflecting climate and forest–soil interactions more than intensive land management (Allen et al., 1998; Huckell, 1996).

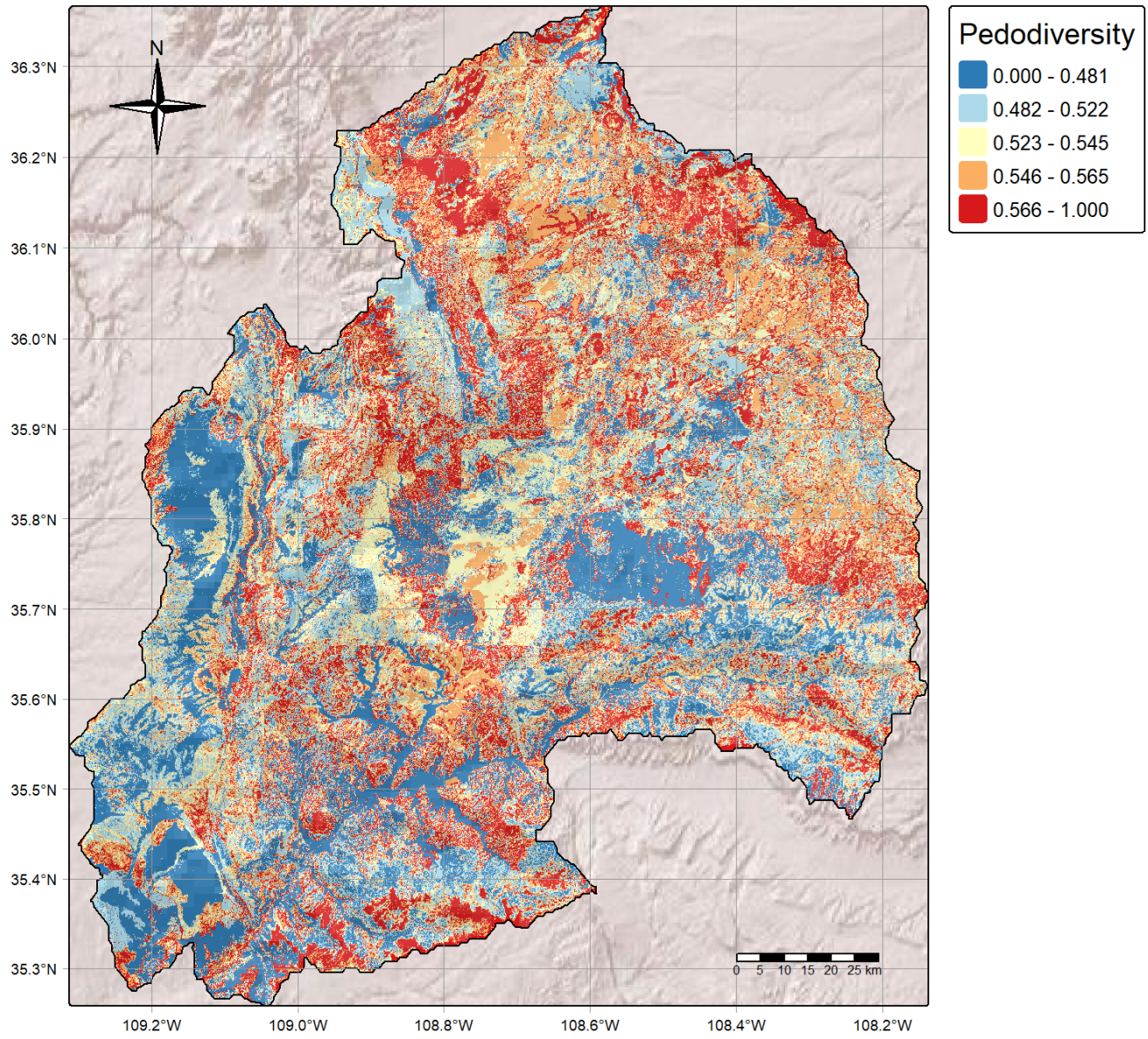

Figure 5: spatial thermodynamic pedodiversity index of the southern Chuska Mountains and southern basin.

Southward, the Chuska Basin transitions to a low-pedodiversity landscape (<0.50) where aeolian sands, episodic rainfall and the shadow of the northern volcanic crest constrain soil development and vegetation complexity (McFadden et al., 1998; Seager et al., 1987). Within this more uniform

terrain, the Navajo pastoral tradition remains sustainable; an ecological adaptation emphasizing mobility, grazing flexibility and stewardship of scarce resources (Redsteer et al., 2018; Weisiger, 2004). The pedodiversity contrast between the mountain flanks and the basin floor thus parallels the entangled relationships of geomorphology, soil formation and cultural adaptation across this sacred and resource-rich landscape (Doolittle, 2000; Pawluk, 1995).

Importantly, this pattern also reflects how differences in soil multifunctionality shaped land-use strategies: high-pedodiversity zones supported diverse cultivation niches, whereas low-pedodiversity soil favored pastoral systems better suited to limited resource options. However, the Chuska landscape exhibits a high degree of patchiness (Gini coefficient = 0.71). Although the reasons for the reorganization of Chaco Canyon around 1100 A.D. remain debated, the unpredictability of these soil niches would likely have made crop production difficult to sustain during periods of environmental stress.

3.2.2 Great Sage Plain

The uplands surrounding the Great Sage Plains, north of Mesa Verde, exhibited moderate pedodiversity values (≈0.48–0.54) across broad loess-covered plains and low-relief valleys (Figure 6). Unlike the deeply incised mesas to the south (Mesa Verde), this landscape consists primarily of Mancos Shale–derived soil mantled by wind-blown silt and fine alluvium, producing gently layered profiles with limited textural contrast (Harden and Taylor, 1983). These conditions favored large, relatively homogeneous fields capable of retaining moisture from seasonal snowmelt, supporting the extensive dryland agriculture practiced by Ancestral Pueblo communities during the later Mesa Verde period (Kohler et al., 2008). Pockets of higher pedodiversity appear along drainage heads and valley margins, where shallow colluvium and slope wash over shale enhanced

local water storage and nutrient heterogeneity. Such microenvironments likely provided greater cropping stability during drought cycles, helping to sustain maize-based agriculture at the northernmost frontier of Ancestral Pueblo settlement (Benson et al., 2007; Ortman, 2016).

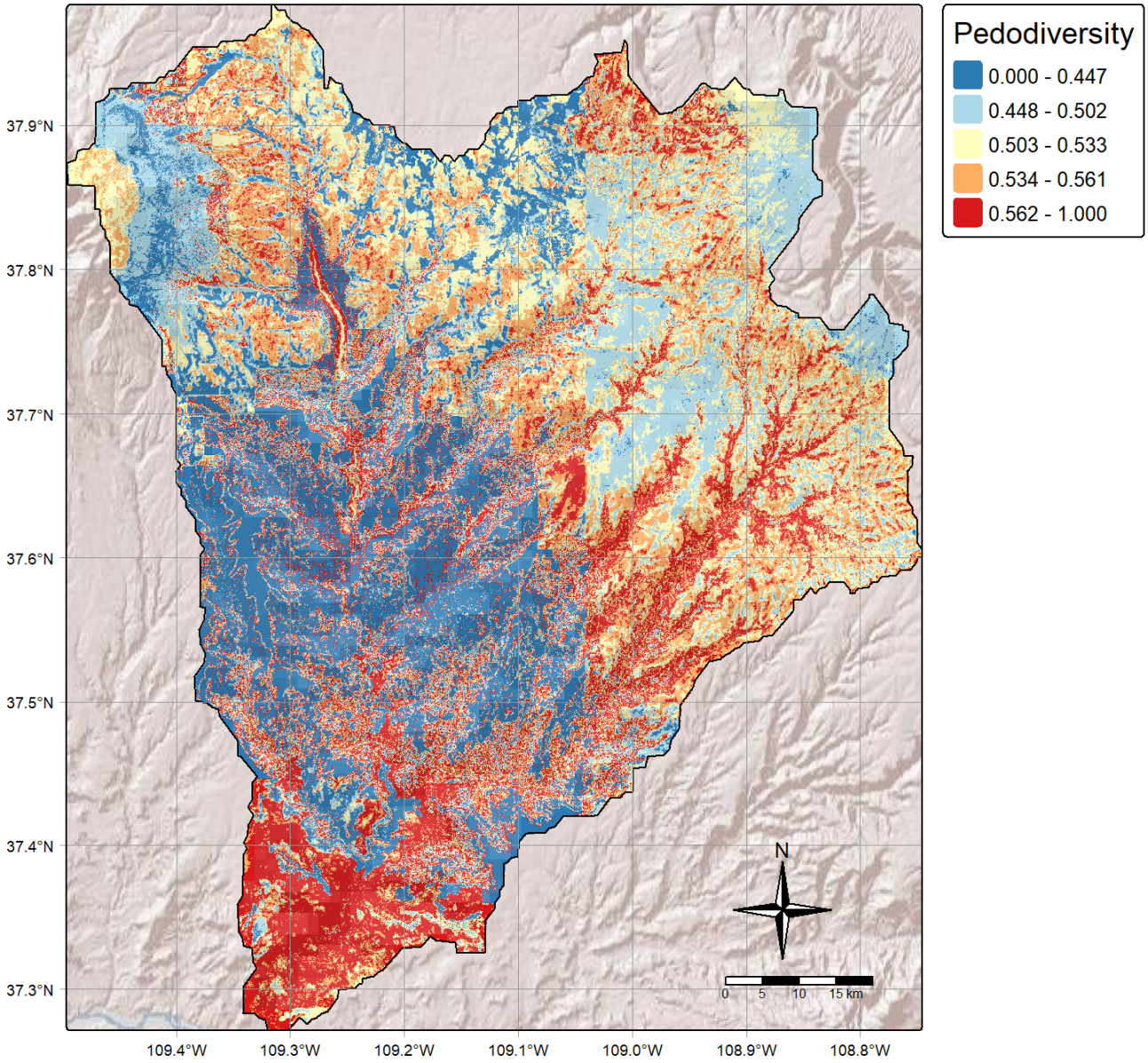

Figure 6: spatial thermodynamic pedodiversity index of the Great Sage Plains on the Colorado and Utah border.

Compared with the high-pedodiversity of the Chuska uplands, where ash-rich parent materials created abundant moisture niches, the Great Sage Plains strength lay in its spatial continuity and

moisture buffering of uniform silty soil, enabling scale and labor efficiency rather than fine-resolution niche exploitation for cultivation (Harden and Taylor, 1983). It represents a functionally productive but less complex agricultural system; however, one more vulnerable to multi-year drought and shortened growing seasons (Benson, 2011). Additionally, the absence of spatial patterns in areas typically assumed to be agricultural land (e.g., fertile valley bottoms) would make soil niches difficult to utilize. The pedodiversity pattern thus helps explain both the intensity of late Ancestral Pueblo farming on the Great Sage Plain (Bocinsky and Kohler, 2014) and the sensitivity of this northern margin to climatic downturns that contributed to regional reorganization in the late 13th century (Benson et al., 2007; Kohler et al., 2008).

3.2.3 Hopi Land

The Hopi Mesas and surrounding uplands exhibit moderate to high pedodiversity values (≈0.52–0.56), concentrated along mesa margins, valley breaks and colluvial footslopes (Figure 7). These areas reflect sandstone and shale parent materials, colluvial reworking and fine-scale topographic variation that together created a variety of soil textures and drainage conditions (Hack, 1942). Such heterogeneity has historically supported the remarkable agricultural and biological diversity of the Hopi landscape, one of North America's longest-inhabited dryland farming regions (Adler, 1996; Cameron, 1999; Whiteley, 2008).

The Hopi cultivate drought-tolerant blue, red and white corns alongside beans, squash, melons and medicinal herbs each adapted to subtle differences in soil conditions (Ferguson and Colwell-Chanthaphonh, 2006; Sekaquaptewa and Washburn, 2004). Areas of elevated pedodiversity correspond closely with traditional field systems where microtopographic and textural diversity enhance soil–water–plant interactions, buffering crops against drought and temperature extremes

(Berkes, 2017). These pedodiversity-rich zones form part of a broader biocultural hotspot, where long-term human stewardship and soil variability together sustain both agro-biodiversity and ecosystem resilience across centuries of arid-land cultivation (Kimmerer, 2013; Müller and Munroe, 2014; Muller et al., 2017).

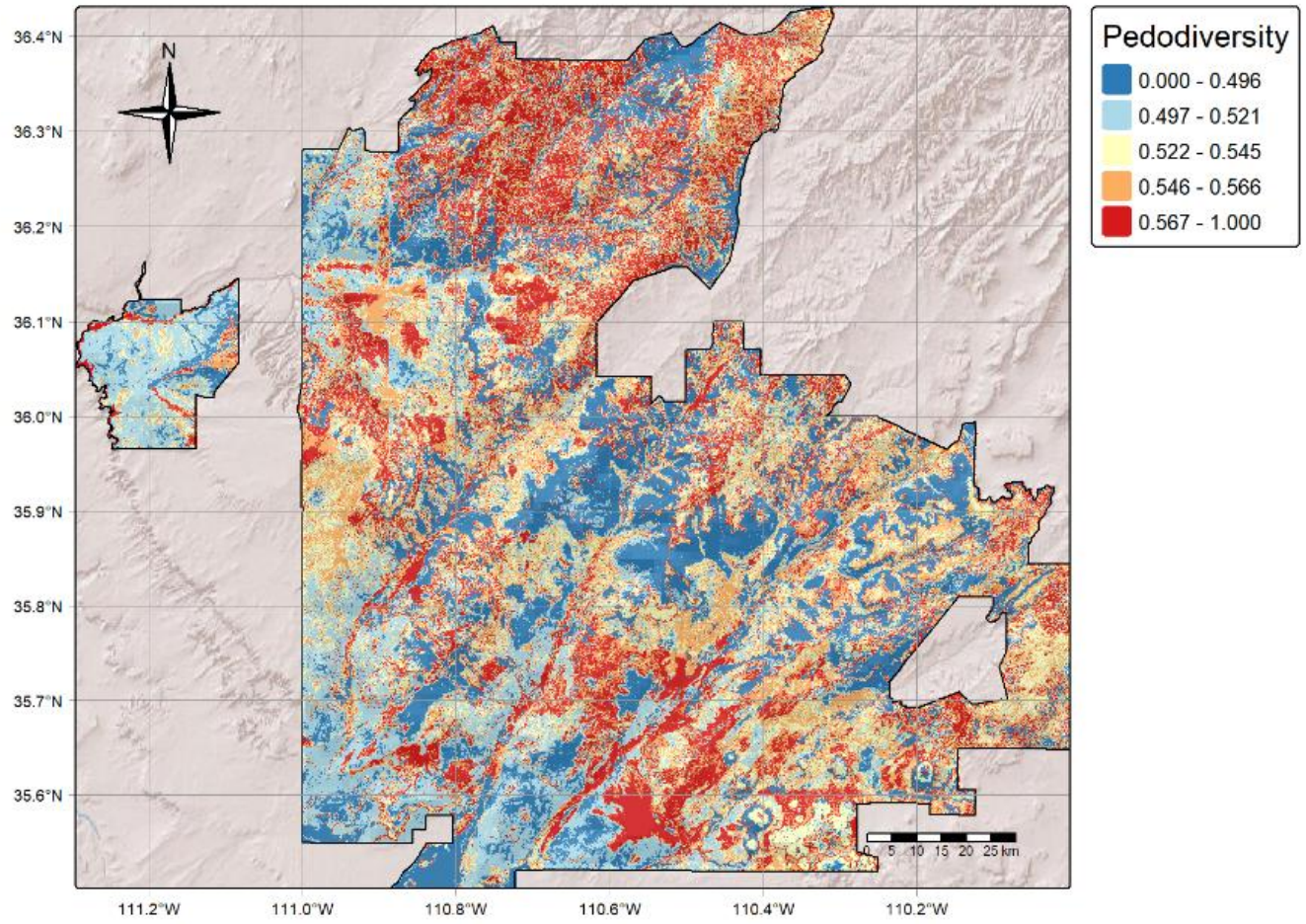

Figure 7: spatial thermodynamic pedodiversity index of the Hopi Land, Arizona.

Across the regions, Hopi Land represent an intermediate position between the high-contrast landscape of the Chuska Mountains and the more homogeneous loessal surface of the Great Sage Plains. However, unlike the steep and climatically stratified Chuska slopes, Hopi soil occurred within a more stable, low-relief plateau environment, where subtle heterogeneity rather than

abrupt contrasts determined the thermodynamic diversity (Hendricks, 1985). It is thought that this caused a relatively more ordered pedodiversity, with clear patterns. The result was a balanced soil structure that sustains both resilience and crop productivity under arid conditions, with knowledge or identifiers of these patterns (Bousselot et al., 2017).

In contrast to the Sage Plain's broad, uniform agricultural surfaces, Hopi fields are intentionally distributed across exergy states ranging from sandy, fast-draining uplands to heavier alluvial footslopes, creating a variety of soil microenvironments that support exceptional agro-biodiversity (Cleveland et al., 1994; Rea, 1997). This adaptability, rooted in the Hopi's knowledge of soil and topographic variation, mirrors the broader pattern observed across the Southwest: an understanding of soil niches and the soil system is often more critical for maintaining a resilient agroecosystem than the absolute level of pedodiversity or whether a culture relies on a crop-dominant or pastoral system (Armstrong et al., 2021; Redsteer et al., 2018). Consequently, pedodiversity is thought to support only a portion of soil multifunctionality, largely independent of cultural factors, though concepts such as pedocomplexity may offer a more integrated perspective.

3.3 Implications and limitations

The framework provides a quantitative bridge between pedodiversity, ecosystem services and food-system resilience. By representing soil as a coupled continuum, the approach identified zones of intrinsic interactions that may serve as biophysical indicators for resilient agriculture and climate adaptation planning with the help of continuous indigenous knowledge (Bünemann et al., 2018; Dominati et al., 2010). The explicit physical formulation also enables integration with a broad range of scientific disciplines from physics to economics, providing a scalable tool for

513 extrapolating resilience potential in contemporary agroecosystems facing intensifying climatic
514 stress. At the fundamental level, it shows the diversity of soil and highlights benefits and possible
515 misconceptions of pedodiversity. However, it is a second-order multidimensional continuous form
516 of the index, which may be difficult to interpret.

517 This study revealed that the spatial pattern of pedodiversity is just as important as pedodiversity
518 itself. Although thermodynamic pedodiversity incorporates multiple dimensions and represents a
519 second-order pedodiversity index, societies with long histories of resilient agriculture appear to
520 have made land-use decisions based on higher-order states beyond pedodiversity alone,
521 consistent with the concept of pedocomplexity. This realization is important both mathematically
522 and philosophically for resilience research. While current approaches move in the right direction,
523 they remain incomplete and require a more rigorous foundation. Integrating mathematical
524 frameworks with Indigenous ecological knowledge will be essential for advancing our
525 understanding of agroecosystem resilience.

526 Therefore, several limitations should be acknowledged. First, this study assumes that societies
527 made land-use decisions primarily to maintain agroecosystem resilience and soil
528 multifunctionality, given the semi-arid, drought-prone environment that necessitates careful
529 management of water, crops, and soils. Sites such as Hopi lands, with continuous cultivation over
530 millennia, or regions with significant Ancestral Pueblo population growth, were selected in part to
531 justify these assumptions. However, this framework does not account for other influencing
532 factors, including agricultural diseases, cultural practices unrelated to agriculture, internal
533 political pressures, geographic constraints, external conflicts and numerous other socio-
534 environmental constraints. While site selection was intended to minimize these confounding
535 influences, it cannot be assumed that all pressures were independent or concurrent. Further

536 research is needed to incorporate these additional dimensions into the pedocomplexity
537 framework.

538 The framework identifies pedodiversity that may correlate with historical land use, but it does not
539 claim to reconstruct the full decision-making, symbolic or social dimensions of Ancestral Pueblo,
540 Navajo or Hopi agricultural systems (Handayani and Prawito, 2010; Kimmerer, 2013). Pedodiversity
541 patterns provide biophysical context, not direct evidence of cultural intent. Moreover, ancestral
542 land use strategies were guided by complex ecological knowledge, spiritual values and
543 multigenerational adaptation that cannot be fully represented by soil processes alone (Berkes,
544 2017; Reo and Whyte, 2012). Interpretations of past agroecosystems should therefore
545 complement, not replace, Indigenous knowledge.

546 The framework measures thermodynamic diversity rather than explicit biological, chemical or
547 agronomic functionality; thus, high pedodiversity does not necessarily equate to high fertility or
548 crop productivity (Nielsen and Wendroth, 2003). Extensive evaluation is required to correlate it
549 with soil morphological, crop yield, function and laboratory analyses in order to realize the full
550 potential of thermodynamic pedodiversity and, ultimately, pedocomplexity. At a fundamental
551 level, it can help explain aspects of soil multifunctionality together with exergy states and latent
552 energy; however, evaluating these innovations requires a comparable level of effort.

553 The use of gridded national soil property datasets (e.g., POLARIS, gNATSURO) introduces
554 uncertainties associated with interpolation and coarse resolution, which may obscure fine-scale
555 heterogeneity that is critical for farm-level decision-making (Chaney et al., 2016). Third, while the
556 biweight convolution provides a realistic finite-support coupling, it assumes isotropic distribution
557 and may underestimate anisotropic behaviors such as preferential flow, layered permeability or

root-mediated transport (Bear, 1972; Jury and Horton, 2004) , all of which can strongly influence agroecosystems.

By quantifying pedodiversity directly through the 3-dimensional Moran's I, we establish a spatially explicit foundation that integrates seamlessly with our broader framework for assessing soil resilience and multifunctionality, providing a mechanistic basis for interpreting how soil structure and management practices interact across heterogeneous Indigenous dryland agroecosystems. Future work should develop a formal mathematical formulation of pedocomplexity and investigate how these thermodynamic states correspond to morphological features on indigenous lands that support resilient agroecosystems.

4 Conclusion

Understanding pedodiversity through a mechanistic, multidimensional framework provides a powerful means of linking soil thermodynamics to landscape scale patterns that support food production and long-term agroecosystem resilience. By quantifying the spatial–vertical variation and rare states of soil processes, this approach identifies zones of high multivariate variability, where thermodynamics broadens the range of soil niche identification. At the same time, it clarifies how societies have historically adapted to these gradients: from the mobile, drought-responsive pastoral systems of the Navajo to the selective crop breeding and field placement strategies of the Hopi that have sustained dryland agriculture for millennia, to the agricultural intensification on more homogeneous soil that may have contributed to the abrupt reorganization of the Mesa Verde Ancestral Pueblo. Most importantly, pedodiversity demonstrates that it is not diversity per se that drives land-use decisions, but the spatial patterns of pedodiversity reflecting

higher-order processes that govern soil resilience and multifunctionality (i.e., pedocomplexity). Modern agricultural and conservation strategies can benefit from recognizing that these soil heterogeneity patterns form the biophysical foundation of productive, resilient food systems, just as they have for Indigenous agroecosystems in the U.S. Southwest. In this way, pedodiversity highlights soil not merely as a substrate for crop production, but as a dynamic archive of human–environment interactions, offering guidance for sustainable farming into the future.

References

Adler, M., 1996. The Prehistoric Pueblo World, A.D. 1150-1350. University of Arizona Press.

Allen, C., Betancourt, J., Swetnam, T., 1998. Landscape changes in the southwestern United States: Techniques, long-term datasets, and trends, in: Perspectives on the Land Use History of North America, Biological Science Report. U.S. Geological Survey, Lafayette, LA, pp. 71–84.

Allison, J., 2010. The End of Farming in the "Northern Periphery" of the Southwest, in: Leaving Mesa Verde: Peril and Change in the Thirteenth-Century Southwest. University of Arizona Press, Tuscon.

Appledorn, C.R., Wright, H.E., 1957. VOLCANIC STRUCTURES IN THE CHUSKA MOUNTAINS, NAVAJO RESERVATION, ARIZONA–NEW MEXICO. Geol Soc America Bull 68, 445. https://doi.org/10.1130/0016-7606(1957)68%255B445:VSITCM%255D2.0.CO;2

Armstrong, C.G., Miller, J.E.D., McAlvay, A.C., Ritchie, P.M., Lepofsky, D., 2021. Historical Indigenous Land-Use Explains Plant Functional Trait Diversity. E&S 26, art6. https://doi.org/10.5751/ES-12322-260206

Arrouays, D., McKenzie, N., Hempel, J., Richer de Forges, A., McBratney, A., 2014. GlobalSoilMap: Basis of the global spatial soil information system, in: Arrouays, D., McKenzie, N., Hempel, J., Richer de Forges, A., McBratney, A.B. (Eds.), . Presented at the 1st GlobalSoilMap Conference, CRC Press, Orleans, France.

Bagley, J.E., Davis, S.C., Georgescu, M., Hussain, M.Z., Miller, J., Nesbitt, S.W., VanLoocke, A., Bernacchi, C.J., 2014. The biophysical link between climate, water, and vegetation in bioenergy agro-ecosystems. Biomass and Bioenergy 71, 187–201. https://doi.org/10.1016/j.biombioe.2014.10.007

Bear, J., 1972. Dynamics of Fluids in a Porous Media. J. Fluid Mech. 61, 206–208. https://doi.org/10.1017/S0022112073210662

Beaton, A.E., Tukey, J.W., 1974. The Fitting of Power Series, Meaning Polynomials, Illustrated on Band-Spectroscopic Data. Technometrics 16, 147–185. https://doi.org/10.1080/00401706.1974.10489171

Bellorado, B.A., Anderson, K.C., 2013. EARLY PUEBLO RESPONSES TO CLIMATE VARIABILITY: FARMING TRADITIONS, LAND TENURE, AND SOCIAL POWER IN THE EASTERN MESA VERDE REGION. KIVA 78, 377–416. https://doi.org/10.1179/0023194013Z.0000000007

Benson, L., 2011. Factors Controlling Pre-Columbian and Early Historic Maize Productivity in the American Southwest, Part 1: The Southern Colorado Plateau and Rio Grande Regions. J Archaeol Method Theory 18, 1–60. https://doi.org/10.1007/s10816-010-9082-z

Benson, L., Cordell, L., Vincent, K., Taylor, H., Stein, J., Farmer, G.L., Futa, K., 2003. Ancient maize from Chacoan great houses: Where was it grown? Proc. Natl. Acad. Sci. U.S.A. 100, 13111–13115. https://doi.org/10.1073/pnas.2135068100

Benson, L., Petersen, K., Stein, J., 2007. Anasazi (Pre-Columbian Native-American) Migrations During The Middle-12Th and Late-13th Centuries – Were they Drought Induced? Climatic Change 83, 187–213. https://doi.org/10.1007/s10584-006-9065-y

Berkes, F., 2017. Sacred Ecology, 4th ed. Routledge. https://doi.org/10.4324/9781315114644

Blagbrough, J.W., 1967. Cenozoic geology of the Chuska Mountains, in: Defiance-Zuni-Mt. Taylor Region, Arizona and New Mexico. Presented at the 18th Annual Fall Field Conference, New Mexico Geological Society, pp. 70–77. https://doi.org/10.56577/FFC-18.70

Bocinsky, R.K., Kohler, T.A., 2014. A 2,000-year reconstruction of the rain-fed maize agricultural niche in the US Southwest. Nat Commun 5, 5618. https://doi.org/10.1038/ncomms6618

Bocinsky, R.K., Varien, M.D., 2017. Comparing Maize Paleoproduction Models with Experimental Data. Journal of Ethnobiology 37, 282–307. https://doi.org/10.2993/0278-0771-37.2.282

Bousselot, J., Muenchrath, D., Knapp, A., Reeder, J., 2017. Emergence and Seedling Characteristics of Maize Native to the Southwestern US. American Journal of Plant Sciences 8. https://doi.org/10.4236/ajps.2017.86087

Breiman, L., 2001. Random Forests (No. 9788578110796). Berkeley, California. https://doi.org/10.1017/CBO9781107415324.004

Brooks, J.F., 2020. Winterthur Portfolio. Henry Francis du Pont Winterthur Museum, Inc. 54, 186–188. https://doi.org/10.1086/711330

Bünemann, E.K., Bongiorno, G., Bai, Z., Creamer, R.E., De Deyn, G., De Goede, R., Fleskens, L., Geissen, V., Kuyper, T.W., Mäder, P., Pulleman, M., Sukkel, W., Van Groenigen, J.W., Brussaard, L., 2018. Soil quality – A critical review. Soil Biology and Biochemistry 120, 105–125. https://doi.org/10.1016/j.soilbio.2018.01.030

Cameron, C.M., 1999. Hopi dwellings: architectural change at Orayvi. University of Arizona Press, Tucson.

Chadwick, O.A., Chorover, J., 2001. The chemistry of pedogenic thresholds. Geoderma 100, 321–353. https://doi.org/10.1016/S0016-7061(01)00027-1

Chaney, N.W., Wood, E.F., McBratney, A.B., Hempel, J.W., Nauman, T.W., Brungard, C.W., Odgers, N.P., 2016. POLARIS: A 30-meter probabilistic soil series map of the contiguous United States. Geoderma 274, 54–67. https://doi.org/10.1016/j.geoderma.2016.03.025

Cleveland, D.A., Soleri, D., Smith, S.E., 1994. Do Folk Crop Varieties Have a Role in Sustainable Agriculture? BioScience 44, 740–751. https://doi.org/10.2307/1312583

Costantini, E.A.C., L'Abate, G., 2016. Beyond the concept of dominant soil: Preserving pedodiversity in upscaling soil maps. Geoderma 271, 243–253. https://doi.org/10.1016/j.geoderma.2015.11.024

Damgaard, C., Weiner, J., 2000. DESCRIBING INEQUALITY IN PLANT SIZE OR FECUNDITY. Ecology 81, 1139–1142. https://doi.org/10.1890/0012-9658(2000)081%255B1139:DIIPSO%255D2.0.CO;2

Dearing, J.A., Wang, R., Zhang, K., Dyke, J.G., Haberl, H., Hossain, Md.S., Langdon, P.G., Lenton, T.M., Raworth, K., Brown, S., Carstensen, J., Cole, M.J., Cornell, S.E., Dawson, T.P., Doncaster, C.P., Eigenbrod, F., Flörke, M., Jeffers, E., Mackay, A.W., Nykvist, B., Poppy, G.M., 2014. Safe and just operating spaces for regional social-ecological systems. Global Environmental Change 28, 227–238. https://doi.org/10.1016/j.gloenvcha.2014.06.012

Dexter, A.R., 2004. Soil physical quality: Part I. Theory, effects of soil texture, density, and organic matter, and effects on root growth. Geoderma 120, 201–214. https://doi.org/10.1016/j.geoderma.2003.09.004

Dominati, E., Patterson, M., Mackay, A., 2010. A framework for classifying and quantifying the natural capital and ecosystem services of soils. Ecological Economics 69, 1858–1868. https://doi.org/10.1016/j.ecolecon.2010.05.002

Dongoske, K.E., Yeatts, M., Anyon, R., Ferguson, T.J., 1997. Archaeological Cultures and Cultural Affiliation: Hopi and Zuni Perspectives in the American Southwest. Am. antiq. 62, 600–608. https://doi.org/10.2307/281880

Doolittle, W.E., 2000. Cultivated Landscapes of Native North America. Oxford University PressOxford. https://doi.org/10.1093/oso/9780198234203.001.0001

Dove, D., Di Naso, S., Gutowski, H., Till, J., Tradlener, L., McBride, B.& D., Gerhardt, K., Flink, P., Dove, D.E., 2006. Topographical Mapping, Geophysical Studies and Archaeological Testing of an Early Pueblo II Village Near Dove Creek, Colorado. https://doi.org/10.6067/XCV87P8XMQ

Duniway, M.C., Herrick, J.E., Monger, H.C., 2010. Spatial and temporal variability of plant-available water in calcium carbonate-cemented soils and consequences for arid ecosystem resilience. Oecologia 163, 215–226. https://doi.org/10.1007/s00442-009-1530-7

Fadem, C.M., Diederichs, S.R., 2020. Farming the Great Sage Plain: Experimental Agroarchaeology and the Basketmaker III Soil Record. Culture Agric Food & Envi 42, 4–15. https://doi.org/10.1111/cuag.12241

Fath, B.D., Patten, B.C., Choi, J.S., 2001. Complementarity of Ecological Goal Functions. Journal of Theoretical Biology 208, 493–506. https://doi.org/10.1006/jtbi.2000.2234

Ferguson, T.J., Colwell-Chanthaphonh, C., 2006. History Is in the Land: Multivocal Tribal Traditions in Arizona's San Pedro Valley. University of Arizona Press.

Gini, C., 1912. Variabilitá e Mulabilitá: Contributo allo Studio delle Distribuzioni edelle Relazioni Statistiche. Bologna: Tipografia di Paolo Cuppini.

Gorelick, N., Hancher, M., Dixon, M., Ilyushchenko, S., Thau, D., Moore, R., 2017. Google Earth Engine: Planetary-scale geospatial analysis for everyone. Remote Sensing of Environment 202, 18–27. https://doi.org/10.1016/j.rse.2017.06.031

Grimm, R., Behrens, T., Märker, M., Elsenbeer, H., 2008. Soil organic carbon concentrations and stocks on Barro Colorado Island — Digital soil mapping using Random Forests analysis. Geoderma 146, 102–113. https://doi.org/10.1016/j.geoderma.2008.05.008

Gustafson, K., Abe, T., 1998. The third boundary condition—was it robin's? The Mathematical Intelligencer 20, 63–71. https://doi.org/10.1007/BF03024402

Hack, J., 1942. The Changing Physical Environment of the Hopi Indians of Arizona. Cambridge, Mass, Reports of the Awatovi expedition, Peabody museum, Harvard university. Report - no. 1, 2.

Handayani, I.P., Prawito, P., 2010. Indigenous Soil Knowledge for Sustainable Agriculture, in: Lichtfouse, E. (Ed.), Sociology, Organic Farming, Climate Change and Soil Science,

Sustainable Agriculture Reviews. Springer Netherlands, Dordrecht, pp. 303–317. https://doi.org/10.1007/978-90-481-3333-8_11
Harden, J.W., Taylor, E.M., 1983. A Quantitative Comparison of Soil Development in Four Climatic Regimes. Quat. res. 20, 342–359. https://doi.org/10.1016/0033-5894(83)90017-0
Harris, A., Schoenwetter, J., Warren, A.H., 1960. An Archaeological Survey of the Chuska Valley and Chaco Plateau New Mexico.
Hendricks, D.M., 1985. Arizona soils. College of Agriculture, University of Arizona, Tucson, Ariz.
Hengl, T., Heuvelink, G.B.M., Stein, A., 2004. A generic framework for spatial prediction of soil variables based on regression-kriging. Geoderma 120, 75–93. https://doi.org/10.1016/j.geoderma.2003.08.018
Hengl, T., Nussbaum, M., Wright, M.N., Heuvelink, G.B.M., Gräler, B., 2018. Random forest as a generic framework for predictive modeling of spatial and spatio-temporal variables. PeerJ 6, e5518. https://doi.org/10.7717/peerj.5518
Hopi Department of Natural Resources, 2021. Climate Change Adaptation Plan for the Hopi Tribe. Hopi Office of Community Planning & Economic Development.
Horn, R., Taubner, H., Wuttke, M., Baumgartl, T., 1994. Soil physical properties related to soil structure. Soil and Tillage Research 30, 187–216. https://doi.org/10.1016/0167-1987(94)90005-1
Huckell, B., 1996. The Archaic Prehistory of the North American Southwest. Journal of World Prehistory 10, 305–373.
Huffman, G., Bolvin, D., Joyce, R., Kelley, O., Nelkin, E., Tan, J., Watters, D., West, J., 2023. Integrated Multi-satellitE Retrievals for GPM (IMERG) Technical Documentation. https://doi.org/10.5067/GPM/IMERG/3B-MONTH/06
Ibán`ez, J.J., De-Albs, S., Bermúdez, F.F., García-Álvarez, A., 1995. Pedodiversity: concepts and measures. CATENA 24, 215–232. https://doi.org/10.1016/0341-8162(95)00028-Q
Ibáñez, J.J., Bockheim, J.G. (Eds.), 2013. Pedodiversity, 0 ed. CRC Press. https://doi.org/10.1201/b14780
Jenny, H., 1941. Factors of Soil Formation: A System of Quantitative Pedology. McGraw- Hill, NY. https://doi.org/10.2307/211491
Jobbágy, E.G., Jackson, R.B., 2000. THE VERTICAL DISTRIBUTION OF SOIL ORGANIC CARBON AND ITS RELATION TO CLIMATE AND VEGETATION. Ecological Applications 10, 423–436. https://doi.org/10.1890/1051-0761(2000)010%255B0423:TVDOSO%255D2.0.CO;2
Johnson, M.K., Rowe, M.J., Lien, A., López-Hoffman, L., 2021. Enhancing integration of Indigenous agricultural knowledge into USDA Natural Resources Conservation Service cost-share initiatives. Journal of Soil and Water Conservation 76, 487–497. https://doi.org/10.2489/jswc.2021.00179
Johnson, T.E., 2023. The Shifting Nature of Subsistence on the Hopi Indian Reservation. Agricultural History 97, 215–244. https://doi.org/10.1215/00021482-10337941
Jost, L., 2006. Entropy and diversity. Oikos 113, 363–375. https://doi.org/10.1111/j.2006.0030-1299.14714.x
Jury, W.A., Horton, R., 2004. Soil physics, 6. ed. ed. Wiley, Hoboken, NJ.
Kahn-John (Diné), M., Koithan, M., 2015. Living in Health, Harmony, and Beauty: The Diné (Navajo) Hózhó Wellness Philosophy. Glob Adv Health Med 4, 24–30. https://doi.org/10.7453/gahmj.2015.044

748 Kim, H., Møller, I., Thorling, L., Hansen, B., 2025. Sediment color as a predictor of the subsurface
749 redox conditions at large scale. Applied Geochemistry 190, 106493.
750 https://doi.org/10.1016/j.apgeochem.2025.106493
751 Kimmerer, R., 2013. Braiding Sweetgrass: Indigenous Wisdom, Scientific Knowledge, and the
752 Teachings of Plants. Environmental Philosophy.
753 Kohler, T.A., Varien, M.D., Wright, A., Kuckelman, K.A., 2008. Mesa Verde Migrations. Am. Sci. 96,
754 146. https://doi.org/10.1511/2008.70.3641
755 Laliberté, E., Zemunik, G., Turner, B.L., 2014. Environmental filtering explains variation in plant
756 diversity along resource gradients. Science 345, 1602–1605.
757 https://doi.org/10.1126/science.1256330
758 Lark, M., 2012. Statistics for Spatio-temporal Data - by Cressie N. & Wikle K.C. European J Soil
759 Science 63, 534–535. https://doi.org/10.1111/j.1365-2389.2012.01473.x
760 Matheron, G., 1963. Principles of geostatistics. Society of Economic Geologists 58, 1246-1266-
761 1246–1266. https://doi.org/10.2113/gsecongeo.58.8.1246
762 McBratney, A., Minasny, B., 2007. On measuring pedodiversity. Geoderma 141, 149–154.
763 https://doi.org/10.1016/j.geoderma.2007.05.012
764 McBratney, A.B., De Gruijter, J.J., Brus, D.J., 1992. Spacial prediction and mapping of continuous
765 soil classes. Geoderma 54, 39–64. https://doi.org/10.1016/0016-7061(92)90097-Q
766 McBratney, A.B., Santos, M.L.M., Minasnya, B., 2003. On digital soil mapping. Geoderma 117, 3–
767 52. https://doi.org/10.1016/S0016-7061(03)00223-4
768 McBrinn, M., Cordell, L., 2016. Archaeology of the Southwest, Third Edition, 3rd ed. Routledge.
769 https://doi.org/10.4324/9781315433738
770 McFadden, L.D., McDonald, E.V., Wells, S.G., Anderson, K., Quade, J., Forman, S.L., 1998. The
771 vesicular layer and carbonate collars of desert soils and pavements: formation, age and
772 relation to climate change. Geomorphology 24, 101–145. https://doi.org/10.1016/S0169-
773 555X(97)00095-0
774 Meyer, H., Reudenbach, C., Hengl, T., Katurji, M., Nauss, T., 2018. Improving performance of
775 spatio-temporal machine learning models using forward feature selection and target-
776 oriented validation. Environmental Modelling & Software 101, 1–9.
777 https://doi.org/10.1016/j.envsoft.2017.12.001
778 Mikhailova, E.A., Zurqani, H.A., Post, C.J., Schlautman, M.A., Post, G.C., 2021. Soil Diversity
779 (Pedodiversity) and Ecosystem Services. Land 10, 288.
780 https://doi.org/10.3390/land10030288
781 Minasny, B., McBratney, A.B., Malone, B.P., Wheeler, I., 2013. Digital Mapping of Soil Carbon, in:
782 Advances in Agronomy. Elsevier, pp. 1–47. https://doi.org/10.1016/B978-0-12-405942-
783 9.00001-3
784 Minasny, B., McBratney, Alex.B., 2016. Digital soil mapping: A brief history and some lessons.
785 Geoderma 264, 301–311. https://doi.org/10.1016/j.geoderma.2015.07.017
786 Moran, P.A.P., 1950. NOTES ON CONTINUOUS STOCHASTIC PHENOMENA. Biometrika 37, 17–23.
787 https://doi.org/10.1093/biomet/37.1-2.17
788 Muhs, D.R., 2017. Evaluation of simple geochemical indicators of aeolian sand provenance: Late
789 Quaternary dune fields of North America revisited. Quaternary Science Reviews 171, 260–
790 296. https://doi.org/10.1016/j.quascirev.2017.07.007
791 Müller, D., Munroe, D.K., 2014. Current and future challenges in land-use science. Journal of Land
792 Use Science 9, 133–142. https://doi.org/10.1080/1747423X.2014.883731

Muller, M.R., Munroe, D.K., Batterman, S.A., 2017. Linking biophysical and cultural dimensions of agroecosystems: Biocultural hotspots in North American drylands. Global Environmental Change 45, 37–49.
Nankar, A.N., Pratt, R.C., 2021. Genotyping by Sequencing Reveals Genetic Relatedness of Southwestern U.S. Blue Maize Landraces. IJMS 22, 3436. https://doi.org/10.3390/ijms22073436
Nielsen, D.R., Wendroth, O., 2003. Spatial and temporal statistics: sampling field soils and their vegetation, GeoEcology Textbook. Catena-Verl, Reiskirchen.
Ortman, S.G., 2016. Uniform Probability Density Analysis and Population History in the Northern Rio Grande. J Archaeol Method Theory 23, 95–126. https://doi.org/10.1007/s10816-014-9227-6
O'Sullivan, R.B., 2003. The Middle Jurassic Entrada Sandstone in northeastern Arizona and adjacent areas, in: Geology of the Zuni Plateau. Presented at the 54th Annual Fall Field Conference, New Mexico Geological Society, pp. 303–308. https://doi.org/10.56577/FFC-54.303
Pawluk, R., 1995. Indigenous knowledge of soil and agriculture at Zuni Pueblo, New Mexico. Iowa State University, Ames, Iowa.
Phillips, J.D., 2007. The perfect landscape. Geomorphology 84, 159–169. https://doi.org/10.1016/j.geomorph.2006.01.039
Press, W.H. (Ed.), 2007. Numerical recipes in Fortran 77: the art of scientific computing, 2. ed., repr.corr. to software version 2.10. ed, Fortran numerical recipes. Cambridge University Press, Cambridge.
Rao, C.R., 1982. Diversity and dissimilarity coefficients: A unified approach. Theoretical Population Biology 21, 24–43. https://doi.org/10.1016/0040-5809(82)90004-1
Rea, A.M., 1997. At the Desert's Green Edge: An Ethnobotany of the Gila River Pima, 1st ed. ed. University of Arizona Press, Erscheinungsort nicht ermittelbar.
Redsteer, M.H., Kelley, K.B., Francis, H., Block, D., 2018. Accounts from Tribal Elders: Increasing Vulnerability of the Navajo People to Drought and Climate Change in the Southwestern United States, in: Nakashima, D., Krupnik, I., Rubis, J.T. (Eds.), Indigenous Knowledge for Climate Change Assessment and Adaptation. Cambridge University Press, pp. 171–187. https://doi.org/10.1017/9781316481066.013
Reheis, M.C., Goldstein, H.L., Reynolds, R.L., Forman, S.L., Mahan, S.A., Carrara, P.E., 2018. Late Quaternary loess and soils on uplands in the Canyonlands and Mesa Verde areas, Utah and Colorado. Quat. res. 89, 718–738. https://doi.org/10.1017/qua.2017.63
Reneau, S.L., McDonald, E.V., Gardner, J.N., Kolbe, T.R., Carney, J.S., Watt, P.M., Longmire, P.A., 1996. Erosion and deposition on the Pajarito Plateau, New Mexico, and implications for geomorphic responses to late Quaternary climatic changes, in: The Jemez Mountains Region. Presented at the 47th Annual Fall Field Conference, New Mexico Geological Society, pp. 391–397. https://doi.org/10.56577/FFC-47.391
Reo, N.J., Whyte, K.P., 2012. Hunting and Morality as Elements of Traditional Ecological Knowledge. Hum Ecol 40, 15–27. https://doi.org/10.1007/s10745-011-9448-1
Rumpel, C., Kögel-Knabner, I., 2011. Deep soil organic matter—a key but poorly understood component of terrestrial C cycle. Plant Soil 338, 143–158. https://doi.org/10.1007/s11104-010-0391-5
Schaetzl, R.J., Anderson, S., 2010. Soils: genesis and geomorphology, 4. print. ed. Cambridge Univ. Press, Cambridge.

Seager, W.R., Hawley, J.W., Kottlowski, F.E., Kelley, S.A., 1987. Geology of east half of Las Cruces and northeast El Paso 1 x 2 sheets, New Mexico. New Mexico Bureau of Geology and Mineral Resources. https://doi.org/10.58799/GM-57

Sekaquaptewa, E., Washburn, D., 2004. *They Go Along Singing* : Reconstructing the Hopi Past from Ritual Metaphors in Song and Image. Am. antiq. 69, 457–486. https://doi.org/10.2307/4128402

Shannon, C.E., 1948. A Mathematical Theory of Communication. Bell System Technical Journal 27, 379–423. https://doi.org/10.1002/j.1538-7305.1948.tb01338.x

Shapiro, S.S., Wilk, M.B., Chen, H.J., 1968. A Comparative Study of Various Tests for Normality. Journal of the American Statistical Association 63, 1343–1372. https://doi.org/10.1080/01621459.1968.10480932

Silverman, B.W., 1986. Density estimation for statistics and data analysis, Monographs on statistics and applied probability. Chapman and Hall, London ; New York.

Soleri, D., Cleveland, D., 1993. Hopi crop diversity and change. Journal of Ethnobiology 13, 203–231.

Stolt, M.H., Ogg, C.M., Baker, J.C., 1994. Strongly Contrasting Redoximorphic Patterns in Virginia Valley and Ridge Paleosols. Soil Science Soc of Amer J 58, 477–484. https://doi.org/10.2136/sssaj1994.03615995005800020033x

Toomanian, N., Esfandiarpoor, I., 2010. Challenges of pedodiversity in soil science. Eurasian Soil Sc. 43, 1486–1502. https://doi.org/10.1134/S1064229310130089

Torrent, J., Schwertmann, U., Schulze, D.G., 1980. Iron oxide mineralogy of some soils of two river terrace sequences in Spain. Geoderma 23, 191–208. https://doi.org/10.1016/0016-7061(80)90002-6

USGS, 2021. Landsat collection 2.

Vivian, R.G., Hilpert, B., 2012. The Chaco Handbook: An Encyclopedia Guide. University of Utah Press.

Vogel, H.-J., Bartke, S., Daedlow, K., Helming, K., Kögel-Knabner, I., Lang, B., Rabot, E., Russell, D., Stößel, B., Weller, U., Wiesmeier, M., Wollschläger, U., 2018. A systemic approach for modeling soil functions. SOIL 4, 83–92. https://doi.org/10.5194/soil-4-83-2018

Wagner, W., Scipal, K., 2000. Large-scale soil moisture mapping in western Africa using the ERS scatterometer. IEEE Transactions on Geoscience and Remote Sensing 38, 1777–1782. https://doi.org/10.1109/36.851761

Walkinshaw, M., 2020. Soil Properties [WWW Document]. California Soil Resource Lab. URL https://casoilresource.lawr.ucdavis.edu/soil-properties/

Wall, D., Masayesva, V., 2004. People of the Corn: Teachings in Hopi Traditional Agriculture, Spirituality, and Sustainability. The American Indian Quarterly 28, 435–453. https://doi.org/10.1353/aiq.2004.0109

Wallace, Z.P., Nielson, R.M., Stahlecker, D.W., DiDonato, G.T., Ruehmann, M.B., Cole, J., 2021. An abundance estimate of free-roaming horses on the Navajo Nation. Rangeland Ecology & Management 74, 100–109. https://doi.org/10.1016/j.rama.2020.10.003

Wang, J.J., 2010. The Chemistry of Soils, Second Edition. Vadose Zone Journal 9, 198–198. https://doi.org/10.2136/vzj2009.0141br

Webster, R., Oliver, M.A., 2007. Geostatistics for Environmental Scientists., 2nd ed, Statistics in Practice. John Wiley & Sons, Inc. https://doi.org/10.2136/vzj2002.0321

Weisiger, M., 2004. The Origins of Navajo Pastoralism. journal of the Southwest 46, 253–282.

Whiteley, P., 2008. Hopi Agriculture and Land Stewardship, in: Fragile Ecologies: The Nature of Nature in Environmental Anthropology. Routledge, pp. 195–212.
Whyte, K.P., 2013. On the role of traditional ecological knowledge as a collaborative concept: a philosophical study. Ecol Process 2, 7. https://doi.org/10.1186/2192-1709-2-7
Wills, W.H., Drake, B.L., Dorshow, W.B., 2014. Prehistoric deforestation at Chaco Canyon? Proc Natl Acad Sci U S A 111, 11584–11591. https://doi.org/10.1073/pnas.1409646111
Zhu, A.X., 1997. A similarity model for representing soil spatial information. Geoderma 77, 217–242.